JOURNAL OF MATERIALS SCIENCE LETTERS 24 (1989) 4057-4061

Thermal shock fracture behaviour of ZrO_2 based ceramics

M. ISHITSUKA, T. SATO, T. ENDO, M. SHIMADA
Department of Applied Chemistry, Faculty of Engineering, Tohoku University, Sendai 980, Japan

Thermal shock fracture behaviour of alumina, mullite, silicon carbide, silicon nitride and various kinds of zirconia based ceramics, such as magnesia partially stabilized zirconia (Mg-PSZ), yttria and ceria doped tetragonal zirconia polycrystals (Y-TZP and Ce-TZP), Y-TZP/Al_2O_3 composites and yttria doped cubic stabilized zirconia (Y-CSZ), was evaluated by the quenching method using water, methyl alcohol and glycerin as quenching media. Thermal shock fracture of all materials seemed to proceed by the thermal stress due to convective heat transfer accompanied by boiling of the solvents under the present experimental conditions. Thermal shock resistance of zirconia based ceramics increased with increasing the fracture strength, but that of Y-TZP and Y-TZP/Al_2O_3 composites was anormalously lower than the predicted value.

1. Introduction

Since ceramic materials show excellent thermal stability and high temperature fracture strength, they have been leading candidates for high temperature structural applications. Thermal shock resistance of ceramic materials is one of the most important properties, because brittle ceramics are susceptible to catastrophic failure under conditions of thermal stress introduced by the temperature difference.

Many studies have been carried out to elucidate the basic principles governing the thermal stress fracture of brittle ceramics. The quenching test into liquid media such as water, silicon oil and liquid metal has been used extensively for characterizing the thermal shock resistance of ceramics [1-3], because this test is relatively simple to provide quantitative thermal shock resistance, e.g. a critical quenching temperature difference, ΔT_c, required the initiation of thermal stress fracture. It was reported [4] that the observed thermal shock resistance was generally in good agreement to the predicted value by the thermal shock resistance parameter, $R = \sigma_f(1 - \nu)/\alpha E$, where σ_f is the fracture strength, ν is Poisson's ratio, α is the linear thermal expansion coefficient and E is Young's modulus.

Since zirconia based ceramics such as Y-TZP show extensively high fracture strength and toughness such as 800-2500 MPa and 7-10 MPa m$^{1/2}$ [5, 6] due to the transformation toughening mechanism, they are expected to show excellent thermal shock resistance. However, thermal shock resistance of zirconia based ceramics were modest [7-11] and the details have not been clarified yet.

In the present paper, the thermal stress fracture behaviour of zirconia based ceramics was evaluated by the quenching method together with that of some other structural ceramics materials.

2. Experimental procedures

Yttria doped tetragonal zirconia powders containing 2 and 3 mol % Y_2O_3 (2Y-TZP and 3Y-TZP), yttria doped cubic stabilized zirconia powder containing 6 mol % Y_2O_3 (6Y-CSZ), ceria doped tetragonal zirconia powders containing 8, 12 and 16 mol % CeO_2 (8Ce-TZP, 12Ce-TZP and 16Ce-TZP), and high purity Al_2O_3 powders were used as starting materials. 2Y-TZP and Al_2O_3 powders were mixed in the desired weight ratio. These powders were isostatically pressed at 200 MPa to form plates (5 mm × 30 mm × 50 mm) and sintered at 1500° C for 3-10 h in air. The presintered samples of 2Y-TZP/Al_2O_3 were hot isostatically pressed at 1450° C and 150 MPa for 1 h in argon atmosphere. The sintered body of mullite was fabricated by the procedures described in the previous paper [10]. The sintered bodies of Mg-PSZ, SiC and Si_3N_4 were supplied by Nilcra Ceramics PTY Ltd, NGK Spark Plug Co., Ltd and Toshiba Co., respectively. The characteristics of the samples are summarized in Table I. The samples were cut into bars (5 mm × 2 mm × 15 mm) and polished to parallel mirror like plane. The thermal shock resistance of each specimen was determined by the quenching test using water, methyl alcohol and glycerin at 0° C as the quenching media. The bending strength (σ_{3b}) of the specimen was determined by 3-point bending test with a crosshead speed of 0.5 mm min^{-1} and span length of 10 mm.

3. Results and discussion

The thermal shock fracture tests of 3Y-TZP and Al_2O_3 were carried out using water, methyl alcohol and glycerin at 0° C as the quenching media. The results are shown in Figs 1 and 2. A variety of the critical temperature differences from 275 to 475° C for 3Y-TZP and 200 to 350° C for Al_2O_3 were observed by using different quenching media.

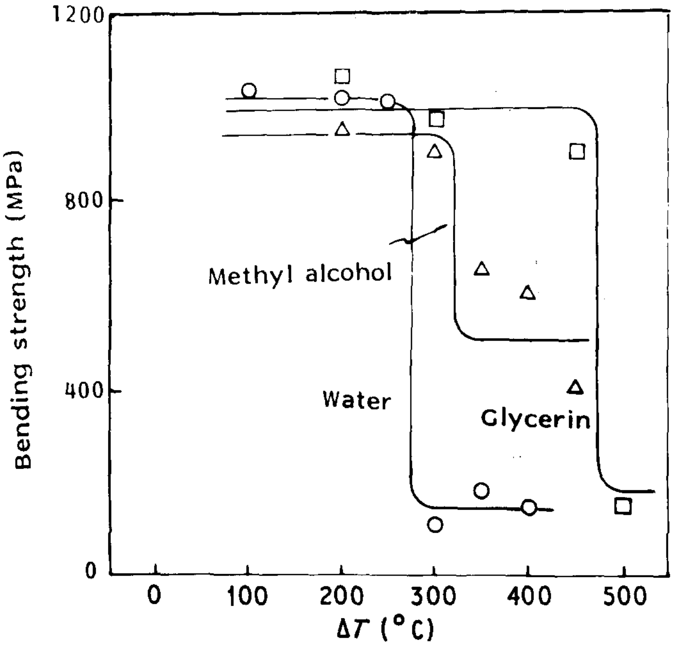

Figure 1 Relation between 3-point bending strength of 3Y-TZP and quenching temperature difference for various quenching media.

Two kinds of heat transfer mechanism, i.e. conductive heat transfer and convective heat transfer, have been considered to interpret the experimental data for thermal shock resistance of ceramics obtained by the quenching test. Analysis of thermal shock resistance is simplified using a nondimensional maximum thermal stresses of σ^* expressed by Equation 1,

$$\sigma^* = S_t(1 - \nu)/\alpha E \Delta T \qquad (1)$$

where S_t and ΔT are the thermal stress and the temperature difference, respectively. When the thermal stress equals the tensile strength, σ_t, of materials, the thermal stress fracture might proceed. Therefore, the critical quenching temperature difference is expressed by Equation 2.

$$\Delta T_c = \sigma_t(1 - \nu)/\alpha E \sigma^* \qquad (2)$$

σ^* for the convective heat transfer, σ_v^*, and conductive heat transfer, σ_d^*, can be described by Equations 3 and 4, respectively [12, 13].

$$1/\sigma_v^* = 1.451(1 + 3.42/\beta)$$
$$= 1.451(1 + 3.42k/r_m h) \qquad (3)$$
$$1/\sigma_d^* = (k_1 \varrho_1 c_1/k_2 \varrho_2 c_2)^{1/2} + 1 \qquad (4)$$

where β is Biot's number, r_m is half thickness for plate sample and radius for cylinder sample, h is heat transfer coefficient, k is thermal conductivity, c is specific heat, ϱ is density and subscripts 1 and 2 refer to the sample and quenching medium, respectively.

The nondimensional thermal stresses, σ_v^* and σ_d^* calculated from Equations 3 and 4 are listed in Table II together with the thermophysical properties of each solvent, where h was calculated by Holman's Equation 5 [14] by assuming natural convection.

$$h = 0.53\,(Gr \cdot Pr)^{1/4}(k_2/2r_m) \qquad (5)$$
$$Gr = gB_2(T_1 - T_2)(2r_m)^3 \varrho_2^2/\mu_2^2$$
$$Pr = c_2\mu_2/k_2$$

where Gr and Pr are Grashof number and Prandtl number, respectively, g is the gravitational constant, B is the volumetric thermal expansion coefficient and μ is the viscosity. The quantity $(T_1 - T_2)$ was taken to be 300° C for all calculations. As seen in Table II, for all quenching media, σ_d^* was greater than σ_v^*. The relationship between ΔT_c and $1/\sigma_d^*$ for 3Y-TZP and Al_2O_3 is shown in Fig. 3. The straight lines were calculated from Equations 2 and 4, where the values of σ_t

TABLE I Characteristics of the sintered bodies

Material	α ($\times 10^{-6}$ K^{-1})	ν	E (GPa)	k (W m^{-1} K^{-1})	σ_{3b} (MPa)	R_0^*
Al_2O_3	7.4	0.27	393	18.5	300	75
SiC	3.2	0.25	330	91	330	234
Si_3N_4	3.2	0.25	330	25	500	355
Mg-PSZ	10.1	0.23	205	1.8	460	171
6Y-CSZ	9.0	0.25	200	3.5	240	100
3Y-TZP	9.0	0.25	200	3.5	900	292
2Y-TZP	9.0	0.25	200	3.5	1300	542
2Y-TZP/10 wt % Al_2O_3	8.8	0.25	229	3.5†	1720	640
2Y-TZP/20 wt % Al_2O_3	8.6	0.26	254	5.7†	2060	698
2Y-TZP/40 wt % Al_2O_3	8.2	0.26	298	7.8†	2070	627
8Ce-TZP	5.2	0.25	200	3.5†	600	433
12Ce-TZP	10.9	0.25	200	3.5†	425	146
16Ce-TZP	5.8	0.25	200	3.5†	160	103

$^*R_0 = \sigma_{3b}(1 - \nu)/\alpha E$
†Estimated

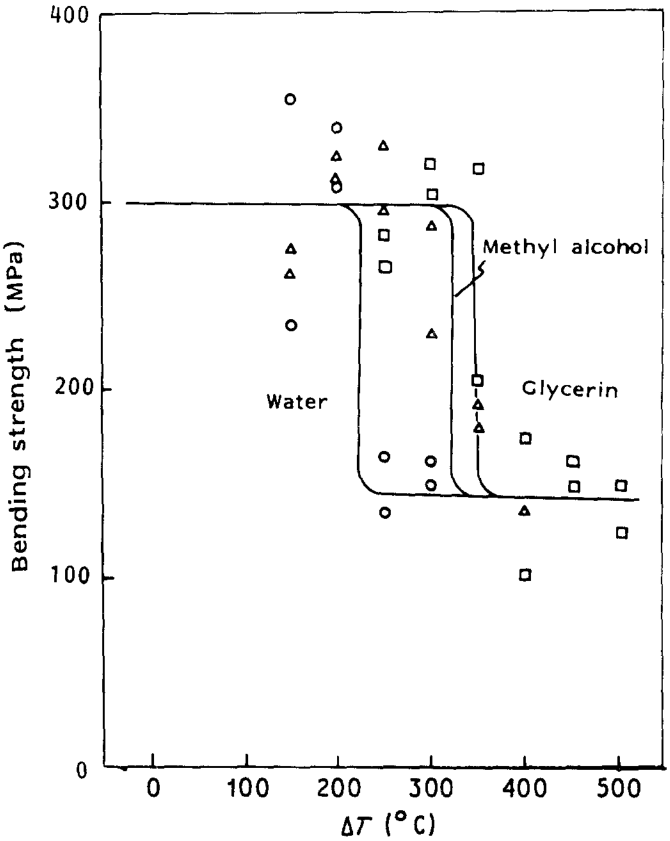

Figure 2 Relation between 3-point bending strength of Al_2O_3 and quenching temperature difference for various quenching media.

were calculated using Equation 6 [15] by using the value of Weibull modulus, m, of 10.

$$\sigma_t/\sigma_{3b} = [1/2(m+1)^2]^{1/m} \tag{6}$$

As seen in Fig. 3, the experimental values were significantly smaller than the calculated ones. These results indicated that thermal shock fracture of the samples was not initiated by the thermal stress due to conductive heat transfer, but the convective heat transfer accompanied by boiling of the solvents played an important role in the thermal stress fracture under these experimental conditions. Actually, it was reported that the heat transfer coefficient under boiling condition was much greater than that under natural convection [16].

ΔT_c of various zirconia based ceramics, Al_2O_3, mullite, SiC and Si_3N_4 determined by the quenching test into water at 0° C are listed in Table III together with 3-point bending strength, σ_{3b}. Since σ_{3b} of TZP and PSZ significantly decreased with increasing temperature, the values of σ_{3b} listed were high temperature 3-point bending strength [6, 17]; σ_{3b}^{h} at 300° C for Mg-PSZ, 3Y-TZP, 2Y-TZP, 2Y-TZP/Al_2O_3 composites and Ce-TZP, and room temperature 3-point bending strength σ_{3b}^{r} for Al_2O_3, SiC and Si_3N_4, where σ_{3b}^{h} for Ce-TZP was estimated by Equation 7.

$$\sigma_{3b}^{h}(\text{Ce-TZP}) = [\sigma_{3b}^{r}(\text{Ce-TZP})/\sigma_{3b}^{r}(\text{2Y-TZP})]\sigma_{3b}^{h}(\text{2Y-TZP}) \tag{7}$$

From Equations 1 and 2, it can be expected that the thermal shock resistance of ceramic materials is improved by increasing fracture strength and by decreasing thermal stress. The relation between σ_{3b}

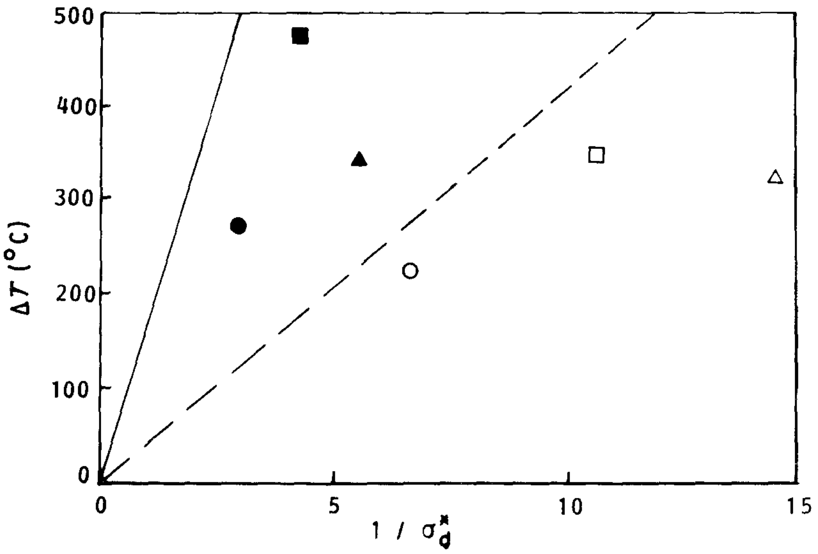

Figure 3 Relation between the critical temperature difference and the reciprocal of the nondimensional maximum stress for conductive heat transfer. Quenching media (○) Al_2O_3 into water, (△) Al_2O_3 into methyl alcohol, (□) Al_2O_3 into glycerin, (●) 3Y-TZP into water, (▲) 3Y-TZP into methyl alcohol, (■) 3Y-TZP into glycerin. σ_t = 400 MPa for Y-TZP and 170 MPa for Al_2O_3.

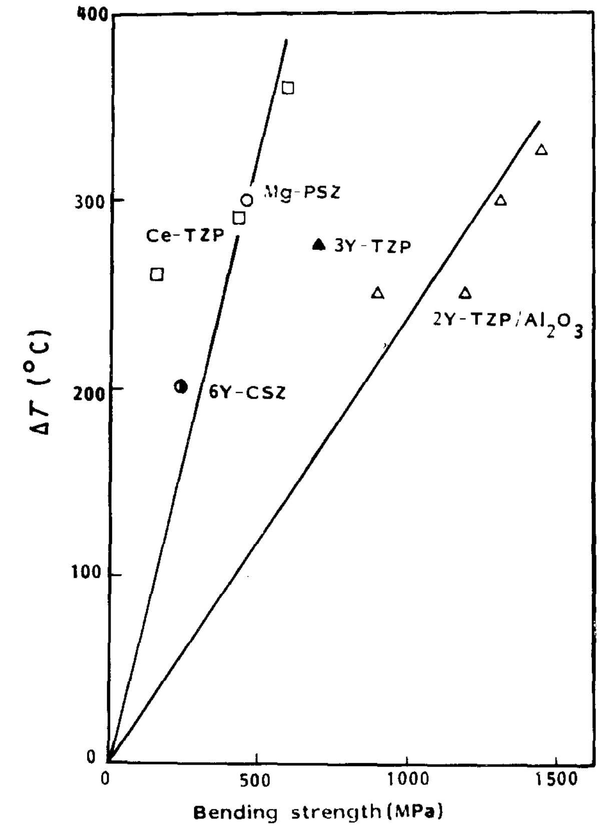

Figure 4 Relation between the fracture strength and the critical water quenching temperature difference of 6Y-CSZ, Mg-PSZ, Ce-TZP, 3Y-TZP and 2Y-TZP/Al_2O_3 composites.

and ΔT_c for zirconia based ceramics is shown in Fig. 4. ΔT_c linearly increased with increasing σ_{3b}, but these plots were divided into two groups. The slope of the straight line for 2Y-TZP, 3Y-TZP and 2Y-TZP/Al_2O_3 composites was noticeably smaller than that for other zirconia ceramics.

TABLE II Characteristic of the solvents, σ_v^*, σ_d^* and ΔT_c of 3Y-TZP and Al_2O_3 in various quenching media

	Methyl alcohol	Glycerin	Water
k ($W m^{-1} K^{-1}$)	0.216	0.285	0.574
$c \times 10^{-3}$ ($J kg^{-1} K^{-1}$)	2.51	2.39	4.20
$\varrho \times 10^3$ ($kg m^{-3}$)	0.792	1.26	1.00
$\mu \times 10^6$ ($kg m^{-1} sec^{-1}$)	0.59	1500	1.79
$B \times 10^6$ (K^{-1})	1700	610	53
σ_v^* (3Y-TZP)	0.167	0.035	0.189
σ_d^* (3Y-TZP)	0.180	0.236	0.341
ΔT_c (3Y-TZP)	350	475	275
σ_v^* (Al_2O_3)	0.017	0.003	0.020
σ_d^* (Al_2O_3)	0.069	0.095	0.150
ΔT_c (Al_2O_3)	350	325	200

$r_m = 2$ mm

Since $k/r_m h$ is positive, Equation 8 can be derived from Equations 2 and 3.

$$\Delta T_c > 1.451\sigma_t(1 - \nu)/\alpha E \qquad (8)$$

The plot of observed ΔT_c against $1.451\sigma_t(1 - \nu)/\alpha E$ is shown in Fig. 5, where σ_t is calculated from Equation 6 using the m of 10. The slope of the dashed line is 1. As expected by Equation 8, the plots of ΔT_c in Ce-TZP, Mg-PSZ, 6Y-CSZ, Al_2O_3, mullite, SiC and Si_3N_4 located above the dashed line, but those of Y-TZP based ceramics such as 3Y-TZP, 2Y-TZP and 2Y-TZP/Al_2O_3 composites were below the dash line.

The heat transfer coefficient, h, calculated by Equations 2 and 3 using the results listed in Table III for Al_2O_3, mullite, SiC, Si_3N_4, Mg-PSZ, 6Y-CSZ and Ce-TZP is shown in Fig. 6 as a function of ΔT_c. The value of h for natural convection calculated by Equation 5 was 1910 $W m^{-2} K^{-1}$ ($\log h = 3.28$). The large value of h in Fig. 6 may be influenced by boiling of the solvents. By assuming the value of $h = 1.0 \times 10^4$ $W m^{-2} K^{-1}$, the thermal fracture stresses of

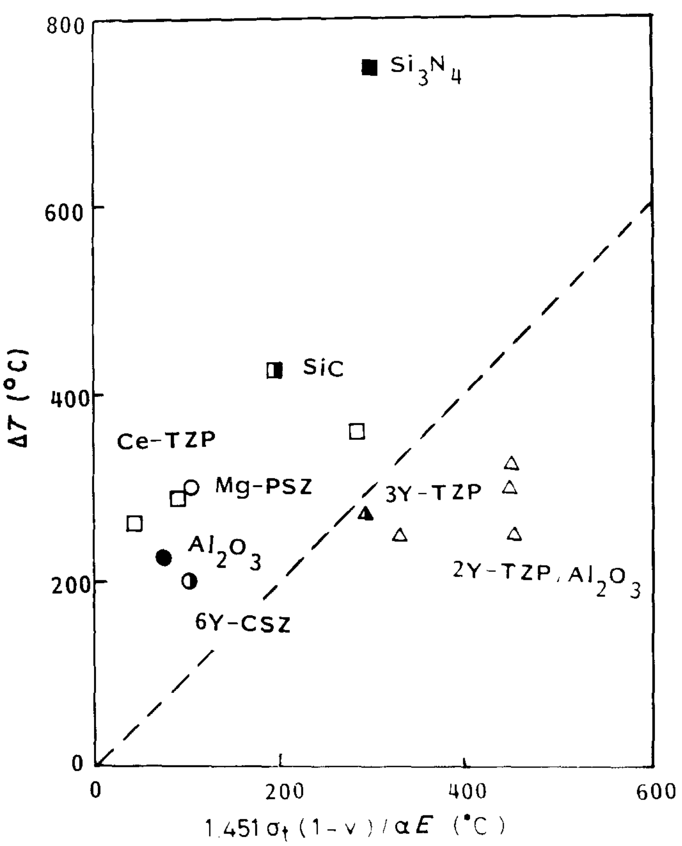

Figure 5 Relation between ΔT_c and thermal shock resistance parameter, $1.451\sigma_t(1 - \nu)/\alpha E$.

TABLE III Bending strength and critical temperature difference of various ceramics quenched into water at 0° C

Material	$\sigma^{\mathrm{r}}_{3\mathrm{b}}$(MPa)	$\sigma^{\mathrm{h}}_{3\mathrm{b}}$(MPa)	ΔT_c(° C)
Al_2O_3	300		225
Si_3N_4	500		750
SiC	330		425
Mg-PSZ	460	353	300
6Y-CSZ	240		200
3Y-TZP	900	700	275
2Y-TZP	1300	900	250
2Y-TZP/10 wt % Al_2O_3	1720	1200	250
2Y-TZP/20 wt % Al_2O_3	2060	1300	300
2Y-TZP/40 wt % Al_2O_3	2070	1450	325
8Ce-TZP	600	439*	360
12Ce-TZP	425	311*	290
16Ce-TZP	160	117*	260

*Estimated

3Y-TZP, 2Y-TZP, 2Y-TZP/Al_2O_3 composites calculated by Equations 1 and 3 were 235–285 MPa. These values were significantly smaller than the fracture strength determined by the bending test. These peculiar results for Y-TZP based ceramics were agreed with the results reported by Ashizuka *et al.* [11].

The present results indicate that the cracks which caused strength degradation in Y-TZP based ceramics were propagated by the thermal stress without the tetragonal to monoclinic phase transformation being smaller than the original fracture stress, because no phase transformation was observed on the surface of the sample quenched from various temperatures into water. Therefore, it seems that the stress-induced phase transformation mechanism does not sufficiently function against thermal stress. However, the detailed mechanism of rapid crack growth without phase transformation in Y-TZP is not clear yet.

4. Conclusion

1. Thermal shock fracture under present experimental conditions was initiated by the thermal stress due to convective heat transfer accompanied by boiling of the solvents.

2. ΔT_c of zirconia based ceramics increased linearly with increasing σ_{3b}, but the thermal shock resistance of Y-TZP based ceramics was anormalously lower than the predicted value.

3. The cracks in Y-TZP based ceramics were propagated by the thermal stress being smaller than the original fracture stress.

Acknowledgement

The authors wish to thank Dr Tsukuma of Toso Co., Ltd, for technical services of HIPing. This work was partly supported by a Grant-in-Aid for Developmental Scientific Research of the Ministry of Education.

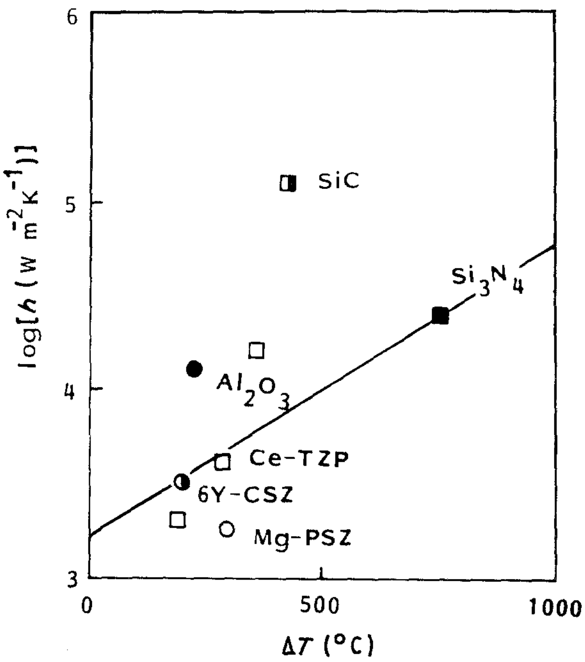

Figure 6 Values of heat transfer coefficient of various ceramics at critical temperature difference.

References

1. D. P. H. HASSELMAN, *J. Amer. Ceram. Soc.* **53** (1970) 490.
2. J. P. SINGH, Y. TREE and D. P. H. HASSELMAN, *J. Mater. Sci.* **16** (1981) 2109.
3. M. OGUMA, C. J. FAIRBANKS and D. P. H. HASSELMAN, *J. Amer. Ceram. Soc.* **69** (1986) C-87.
4. D. LEWIS, *ibid.* **63** (1980) 713.
5. K. TSUKUMA and M. SHIMADA, *Amer. Ceram. Soc. Bull.* **64** (1985) 310.
6. K. TSUKUMA, K. UEDA, K. MATSUSHITA and M. SHIMADA, *J. Amer. Čeram. Soc.* **68** (1985) C-54.
7. M. V. SWAIN, *J. Mater. Sci. Lett.* **2** (1983) 279.
8. T. SATO, T. FUKUSHIMA, T. ENDO and M. SHIMADA, *ibid.* **6** (1987) 1287.
9. A. H. HEUER and L. H. SCHOENLEIN, *J. Mater. Sci.* **20** (1985) 3421.
10. M. ISHITSUKA, T. SATO, T. ENDO and M. SHIMADA, *J. Amer. Ceram. Soc.* **70** (1987) C-342.
11. M. ASHIZUKA, Y. KIMURA, H. FUJII, K. ABE and Y. KUBOTA, *J. Ceram. Soc. Jpn* **94** (1986) 577.
12. J. P. SINGH, J. R. THOMAS and D. P. H. HASSELMAN, *J. Amer. Ceram. Soc.* **63** (1980) 140.
13. H. HENCKE, J. R. THOMAS and D. P. H. HASSELMAN, *ibid.* **67** (1984) 393.
14. J. P. HOLMAN, "Heat Transfer", 3rd edition (McGraw-Hill, New York, 1981).
15. D. G. S. DAVIS, *Proc. Brit. Ceram. Soc.* **22** (1973) 429.
16. S. NUKIYAMA, *Nippon Kikai Gakkai-shi* **37** (1934) 367.
17. K. TSUKUMA, Y. KUBOTA and T. TSUKIDATE, *FC Report* **1** (1983) 8.

Received 9 June and accepted 7 December 1988